Quantitative Analysis of Star-Branched Polymers by Multidetector Size-Exclusion Chromatography

STEPHEN T. BALKE,[1] THOMAS H. MOUREY,[2] DOUGLAS R. ROBELLO,[2] TAMMY A. DAVIS,[2] ALEXANDER KRAUS,[2,*] KRZYSZTOF SKONIECZNY[1]

[1] Department of Chemical Engineering and Applied Chemistry, University of Toronto, Toronto, Ontario M5S 3E5, Canada

[2] Imaging Materials and Media—Research and Development, Eastman Kodak Company, Rochester, New York 14650-2136

Received 24 May 2001; accepted 17 September 2001

ABSTRACT: The object of this study is to develop multidetector size-exclusion chromatography (SEC) methods to determine the number of arms per molecule across the molecular size distribution of star-branched polymers. An empirical fit between the intrinsic viscosity molecular contraction factor g' and the number of arms f is used as an alternative to converting g' values to root mean square radii ratios used by random walk models. The quantitative analysis of star polymer distributions by SEC is then reduced to understanding factors unique to the accurate measurement of g' across the molecular size distribution. Two methods of analyzing SEC data are then tested: (1) the "conventional method" utilizing values of weight-average molecular weight and intrinsic viscosity at each retention volume and (2) the method of component chromatograms. The latter is a new method useful when only a few different types of branching are present. It depends on fitting each detector's chromatograms as the sum of component chromatograms. Plotting the intrinsic viscosity of the branched polymer versus that of the linear polymer at the same molecular weight was useful for diagnosing problems. The conventional method was defeated by axial dispersion in the narrow chromatograms and the homogeneity of branching in the samples. The component chromatogram method avoids the axial dispersion problem but its value depends on how accurately the component peaks reflected the true situation. In this study, the method provided the most reasonable values when component peaks were grouped together. © 2002 Wiley Periodicals, Inc. J Appl Polym Sci 85: 552–570, 2002

Key words: star-branched polymer; intrinsic vicosity; size-exclusion chromatography; component chromatogram; molecular size distribution; molecular weight polydispersity

INTRODUCTION

There has been increasing interest in polymers with branched structures because the presence of branches can lead to highly desirable physical properties.[1] Among the possible variations of branched polymers, *star polymers* are a special case,[2] distinguished by a structure containing many chains radiating from a relatively compact core. Star polymers have been synthesized both by anionic[3,4] and cationic[5,6] polymerization, but more recently living radical polymerization techniques have been employed.[7–9] These newer

Correspondence to: S. T. Balke.
**Present address:* Degussa Construction Chemicals Germany, Dr.-Albert-Frank-Str. 32, 83308 Trostberg, Germany.

Journal of Applied Polymer Science, Vol. 85, 552–570 (2002)

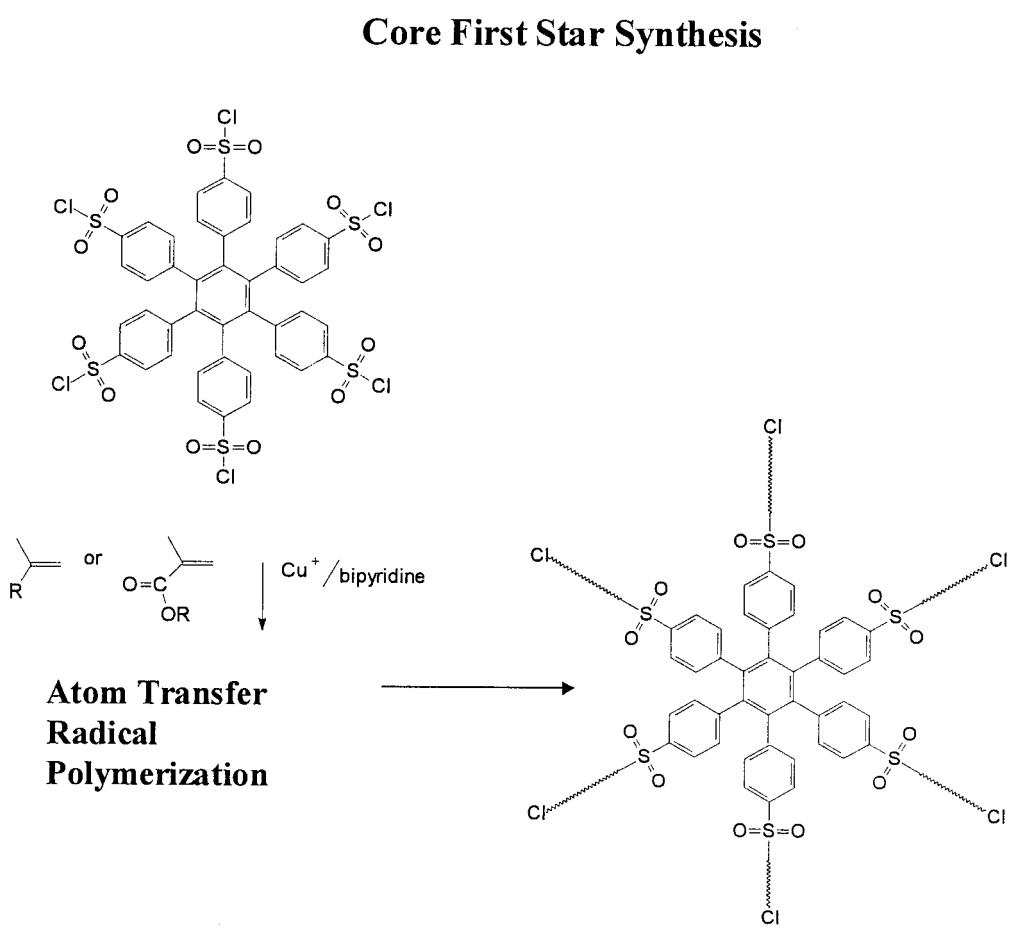

Figure 1 Schematic diagram of the "core first" method of atom transfer radical polymerization.

methods of synthesis are expected to facilitate the production of increasingly complicated star and other branched polymers tailored for specific applications.

The topic of this study is the quantitative analysis of star-branched poly(methyl methacrylate) (PMMA) using a size-exclusion chromatograph equipped with refractometer detector, a differential viscometer, and a two-angle laser light-scattering detector. The objective is to develop methods of using multidetector size-exclusion chromatography (SEC) to determine the number of arms per molecule across the molecular size distribution of star-branched polymers. In the following section, the complexities associated with accomplishing this objective are detailed. Then two methods of interpretation are shown. The first is the conventional method, based on evaluation of weight-average molecular weight M_w and intrinsic viscosity $[\eta]$ at each retention volume (i.e., "local" property values). The second is a new method termed the component chromatogram method.

THEORY

Star polymers were produced by a version of living radical polymerization, atom transfer radical polymerization (ATRP),[10] using multifunctional core molecules[11] with sulfonyl chloride initiating groups[12] and a copper (I) catalyst. The general synthetic scheme is known as the *core-first* approach (Fig. 1), and is exemplified by the synthesis of six-arm poly(methyl methacrylate) (PMMA). Ideally, each arm grows independently from the core, to produce a homogeneous polymer containing precisely six arms and with a narrow distribution of arm lengths. However, in practice, the initiators are not completely pure; some of the sulfonyl chloride groups may be hydrolyzed by adventitious water. In addition, initiation may

not be complete for all sites because of steric crowding. These nonideal behaviors produce some core molecules with fewer than the desired number of initiating sites, and lead to star polymers with "amputated" arms. In addition, none of the living radical polymerization methods, including ATRP, provides perfect control. A minor amount of termination inevitably occurs, resulting in stars with shortened arms or, in the case of termination, by radical–radical coupling, doublet, triplet, or higher stars clusters. These coupling reactions become more noticeable either when the polymerization reaction is carried out to high conversion or when the functionality of the core molecule is very large.[9] Adding to this complexity is that the by-products as well as the main product are expected to possess narrow molecular weight distributions. However, a relatively small set of discrete by-products is usually present.

Conventional multidetector SEC interpretation is most well developed for the case of linear homopolymers, and broad molecular weight distributions with an uninterrupted, continuous variety of different molecular weights. For these types of samples, an "effective" interdetector volume has proven very useful for dealing with the combined interdetector volume/axial dispersion correction problem.[13] This method cannot be employed for narrow molecular weight distributions. A separate specification of "true" interdetector volume and correction of axial dispersion is then necessary. Results are very sensitive to even small errors and the general situation of multidetector SEC interpretation of narrow molecular weight distribution samples is quite unsatisfactory. A partial solution is obtained by calculating from the data only average quantities such as the weight-average molecular weight and intrinsic viscosity of the whole sample that can be obtained from each detector independently of any other. However, for mixtures of stars and by-products this alternative does not currently enable the number of arms in the primary product to be determined across the molecular size distribution.

This study examines two methods for determining the number of arms per molecule from the SEC data. The first is the *conventional approach,* in which the "true interdetector volume" and a separate axial dispersion correction are used. This approach assumes a continuous variety of different polymer molecules (differing in molecular weight and/or branching) across the chromatogram and is expected to become increasingly difficult to implement as the variety decreases. A mixture of a few types of stars, each with a narrow molecular weight distribution, is the worst case for the conventional method. The second method is a new one, termed the *component chromatogram method,* and is an exact complement to the conventional method. It is best used for a mixture of a few types of stars, each with a narrow molecular weight distribution, and it is less effective when there is a continuous variety of polymer molecules in the sample. These two methods each provide the intrinsic viscosity and the weight-average molecular weight for the molecules of interest. They share a common method of interpretation to obtain the number of arms per molecule from this information. This commonality is described in the next section, after which each of the two methods is described in turn.

Number of Arms per Molecule from Intrinsic Viscosity and Weight-Average Molecular Weight

A recent review[14] provides an excellent summary of the current state of analysis of stars using dilute solution methods. It is evident that many alternatives are available. A fundamental approach to the problem is to base the analysis on the ratio of the radii of gyration of branched and linear molecules of the same molecular weight (the molecular contraction "g factor"). The basic principles are extended to SEC chromatograms by measuring the molecular contraction factor at each retention volume, providing detailed information on star conformation across the molecular size distribution. This distribution information is unique to SEC and cannot be obtained directly by classical methods that measure average properties of unfractionated, whole polymer samples. However, although obtainable from SEC–multiangle light-scattering detectors, often in practice and in particular for the samples examined here, root mean square radii are too small to be measured accurately and precisely over the entire molecular size distribution. Instead, the interpretation developed here centers on the use of ratio of intrinsic viscosities (the "g' factor"), defined as follows:

$$g_i' = \left(\frac{[\eta]_i}{[\eta]_{\mathrm{lin},i}} \right)_{M_{w,i}} \tag{1}$$

and

$$[\eta]_{\text{lin},i} = K_w M_{w,i}^a \tag{2}$$

where the subscript i refers to the ith type of molecule present in the product. If a continuous variety of molecules is assumed, then this is the same as the value at the retention volume v_i. The intrinsic viscosity can be measured at each retention volume by SEC–viscometry detectors, even at very small molecular sizes, and provides greater latitude for the analysis of star polymers than SEC–light-scattering detectors. However, the relationship between the intrinsic viscosity molecular contraction factor g' and the number of arms has a more uncertain theoretical basis than models such as the random walk approach of Zimm and Stockmayer,[15] which predicts

$$g_{rw} = \frac{3f - 2}{f^2} \tag{3}$$

where the subscript rw indicates that this g is the theoretical random walk value and f is the number of arms for the star. This equation is of very limited application and is valid only for regular stars (all arms of the same length) under theta conditions. In this work it is used only to provide a comparison with actual experimental values. It also requires some estimation of g from g' values. In the case of measurements from SEC–viscometry, g is often related to g' by using

$$g' = g^{\varepsilon} \tag{4}$$

Jackson et al.[16] recently found that a value of 0.79 for the constant ϵ appeared reasonable for polystyrene stars in tetrahydrofuran (THF). The theoretical value is $\epsilon = 0.5$ in a theta solvent and values are dependent on solvent and star composition. This uncertainty in ϵ creates an unsettling uncertainty in f from eq. (3), not including the underlying limitations of the random walk prediction. For example, ϵ values of 0.5 and 0.79, respectively, predict 5.5 versus 4 arms for $g' = 0.69$ and 7.9 versus 5.1 arms for $g' = 0.59$. In addition, the value of ϵ can vary across the molecular size distribution. In some instances ϵ can be measured by SEC–multiangle light-scattering detection, but as mentioned previously, the entire root mean square radius distribution is often not accessible to this detection method, and at some lower size limit an estimated value of ϵ is required.

Another way of examining SEC data can utilize eq. (1) written as

$$\log[\eta]_{\text{br},i} = \log [\eta]_{\text{lin},i} + \log g' \tag{5}$$

so that a plot of $\log[\eta]_{br,i}$ versus $\log[\eta]_{\text{lin},i}$ will be a straight line with a slope of unity and an intercept of $\log g'$. Because g' depends on f, parallel lines are to be expected for different values of f.

In this study, rather than rely on the adequacy of the random walk assumption and the uncertainty in converting g' to g using estimated values of ϵ, an empirical approach is used. Literature data provide the parallel lines based on eq. (5) at various specific values of f. These lines, in turn, provide values of g' that can then be correlated with f. Values of g' at other f values are then interpolated, with the result that a parallel line following eq. (5) can be plotted for every value of f. It will be shown that the uncertainty in predicting the number of arms f from values of g' by the empirical fit is potentially better than using estimated values of ϵ and eq. (4), regardless of solvent quality. The result then is that two correlations provide the means for deriving f from SEC data: a plot of g' versus f and a plot of $\log[\eta]_{br,i}$ versus $\log \log[\eta]_{\text{lin},i}$ for each f (referred to here as a $[\eta]_{br,i}$–$[\eta]_{\text{lin},i}$ plot).

The Conventional Approach

In the conventional approach, the "true interdetector volume" is obtained by injecting small molecules and observing the differences in the peak retention volumes between detectors. Local values of intrinsic viscosity are calculated from

$$[\eta]_i = \frac{\eta_{sp,i}}{c_i} \tag{6}$$

and local values of M_w from

$$M_{w,i} = \frac{1}{P(\theta)\left(\dfrac{K_{\text{LS}} c_i}{R(\theta)_i} - 2A_2 c_i\right)} \tag{7}$$

where

$$K_{\text{LS}} = \frac{2\pi^2 (n_0)^2 (dn/dc)^2 (1 + \cos^2\theta)}{\lambda^4 \times 6.02252 \times 10^{23}} \tag{8}$$

where λ is the wavelength of the laser light-scattering source, n_0 is the refractive index of the solvent, and (dn/dc) is the specific refractive index increment.

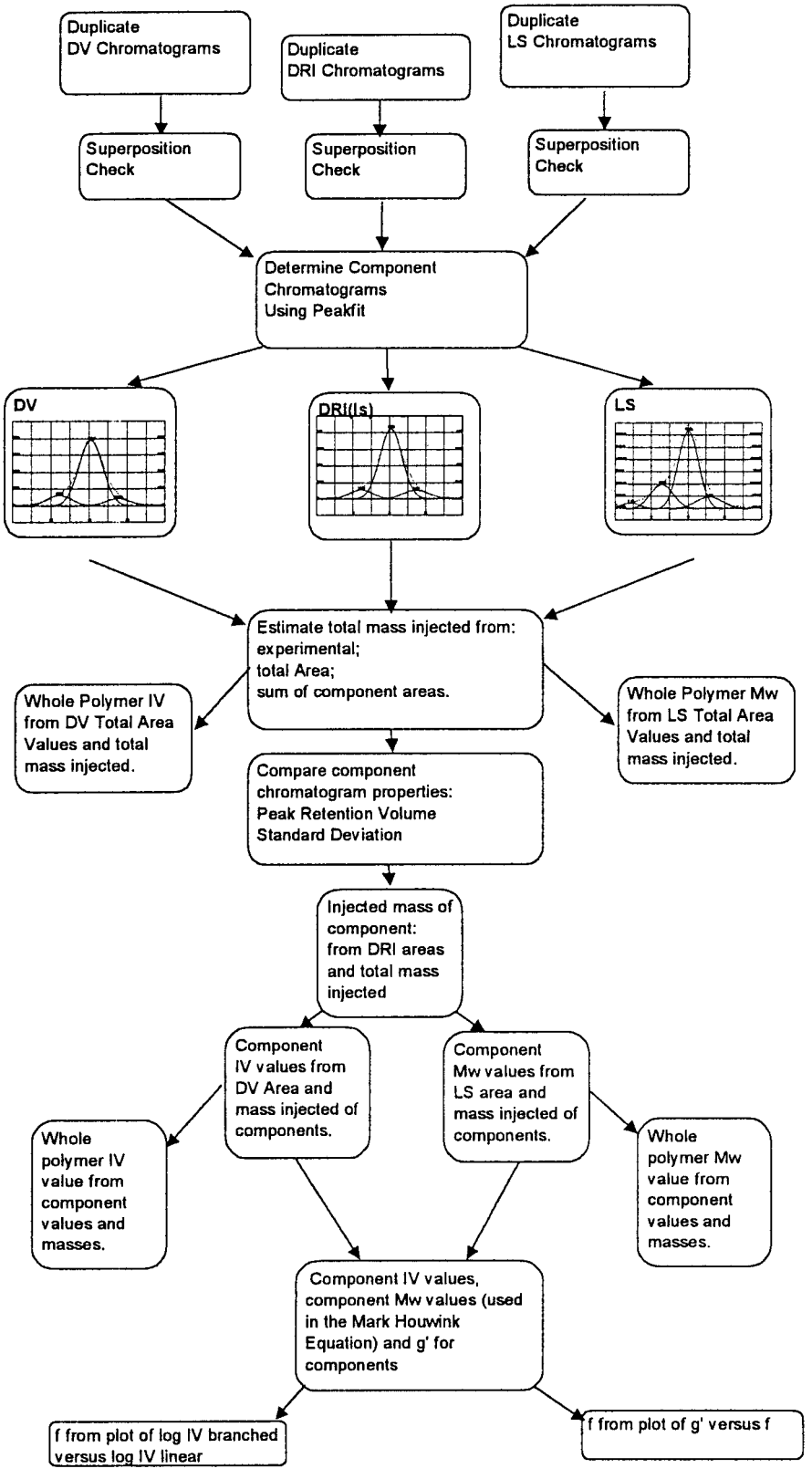

Figure 2 Schematic flow diagram of the "component chromatogram method."

Table I g' Values

Reference for g'_{exp}	f	g'_{exp}	g' This Study	Theoretical g' [eqs. (3) and (4)]	Empirical Fits	
					g' eqs. (22)	g' eqs. (23)
	2	1	1	1.000	0.997	
20	3	0.84	0.835	0.820	0.842	
21	4	0.724	0.726	0.690	0.730	
22	4	0.733	0.738	0.690	0.730	
	5			0.597	0.649	
22	6	0.589	0.592	0.527	0.593	0.587
	7			0.473		0.541
	8			0.430		0.498
	9			0.395		0.459
	10			0.366		0.422
	11			0.341		0.389
20	12	0.34	0.352	0.320		0.358
	13			0.301		0.330
	14			0.285		0.304
	15			0.271		0.279
	16			0.258		0.257
	17			0.246		0.237
23	18	0.225	0.22	0.236		0.218
24	32	0.154	0.149	0.152		
25	64	0.09	0.086	0.088		
25	128	0.05	0.044	0.051		
26	270	0.03	0.043	0.029		
26	270	0.025	0.042	0.029		

The local weight-average molecular weight and local intrinsic viscosities can then each be corrected for the effects of axial dispersion by using the equations developed by Hamielec.[17] Assuming that axial dispersion causes molecules of each i molecular size to form a Gaussian chromatogram of constant standard deviation σ, and that the molecular weight calibration curve is linear, Hamielec derived the following equations to correct local M_w ($M_{w,i}$) and local $[\eta]$ ($[\eta]_i$) for the effects of axial dispersion.

$$\frac{M_{w,i}(uc)}{M_{w,i}(c)} = \frac{F(v - D_2\sigma^2)}{F(v)} \exp\left(\frac{(D_2\sigma)^2}{2}\right) \quad (9)$$

$$\frac{[\eta]_i(uc)}{[\eta]_i(c)} = \frac{F(v - D_{2\eta}\sigma^2)}{F(v)} \exp\left(\frac{(D_{2\eta}\sigma)^2}{2}\right) \quad (10)$$

where (c) denotes the axial dispersion corrected value and (uc) denotes the value uncorrected for axial dispersion; F is the function yielding the height of the nonnormalized DRI chromatogram; D_2 is the slope of the molecular weight calibration curve (plotted as ln M versus retention volume v); and $D_{2\eta}$ is the slope of the intrinsic viscosity calibration curve (plotted as ln$[\eta]$ versus retention volume v).

Using eqs. (9) and (10), the "true" $M_{w,i}$ and $[\eta]_i$ at each retention volume can be obtained. Using the Mark–Houwink equation to obtain the $[\eta]_i$ for a linear polymer of local weight-average molecular weight $M_{w,i}$ at each point , g' can be calculated from eq. (1), for each retention volume across the total chromatogram.

The Component Chromatogram Method

This method involves fitting each of the three chromatograms from the multidetector system as the sum of j component chromatograms. The component chromatograms are each treated as a homogeneous polymer with the chromatogram areas yielding estimates of whole polymer intrinsic viscosities and the weight-average molecular weight of each component. Along with the results of analysis of linear polymers, these data provide the ratio of intrinsic viscosities of branched and linear material at the same molecular weight (g')

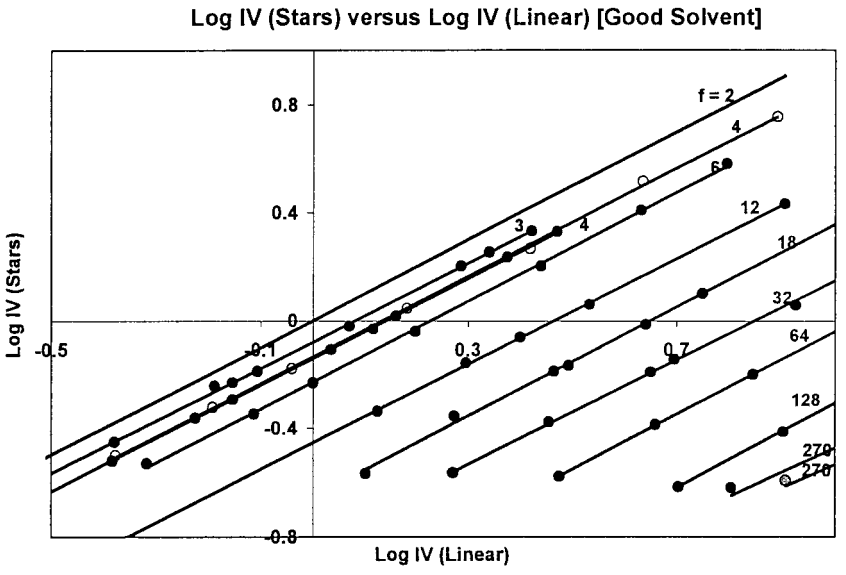

Figure 3 Logarithm of intrinsic viscosity of the star-branched polymer versus logarithm of intrinsic viscosity of the linear polymer of the same molecular weight using data from published literature (see Table I for the values of g' and the references). Each line corresponds to a different number of arms (f).

to permit application of various methods for calculating the number of arms. Figure 2 shows a schematic diagram of the method including computations necessary to check for random or systematic error. Calculated errors need to be compared to values that are considered acceptable for the specific SEC system. Using Figure 2 as a guide, the method is summarized as follows:

1. The data input to the method consists of chromatograms from duplicate SEC runs on an instrument having a differential refractive index (DRI), differential viscometer (DV), and light-scattering (LS) detector. Thus, three different types of chromatograms are obtained.
2. Superposition check refers to the usual chromatographic assessment of how valid are the raw data. Duplicate chromatograms are superimposed on each other and, if superposition is judged unsatisfactory (which could happen for a wide variety of reasons, ranging from a change in chromatograph operating variables to inadequate baseline drawing), the data are not used.
3. Determine component chromatograms. A software program (Peakfit; SPSS Inc., Chicago, IL) is used to fit the input chromatograms as the sum of component Gaussian chromatograms.
4. Estimate total mass injected. Three estimates of total mass injected are associated with each DRI chromatogram. The first estimate is the experimental value m_{exp}, obtained from knowledge of the concentration of solution injected and the volume injected.

The second estimate, m_{tarea}, is obtained from multiplying the total area under the DRI chromatogram by the detector response constant.

$$m_{\text{tarea}} = \kappa \int_0^\infty W(v)\, dv = \int_0^\infty c(v)\, dv \qquad (11)$$

where κ is the detector response constant; $W(v)$ is the nonnormalized detector response from the DRI detector; and $c(v)$, the product of κ and $W(v)$, is the concentration of polymer at each retention volume.

The third estimate, m_{carea}, is obtained by summing the areas under the component peaks and multiplying them by the detector response constant.

$$m_{\text{carea}} = \sum_{j=1}^{n} \kappa_j A_{\text{DRI},j} \qquad (12)$$

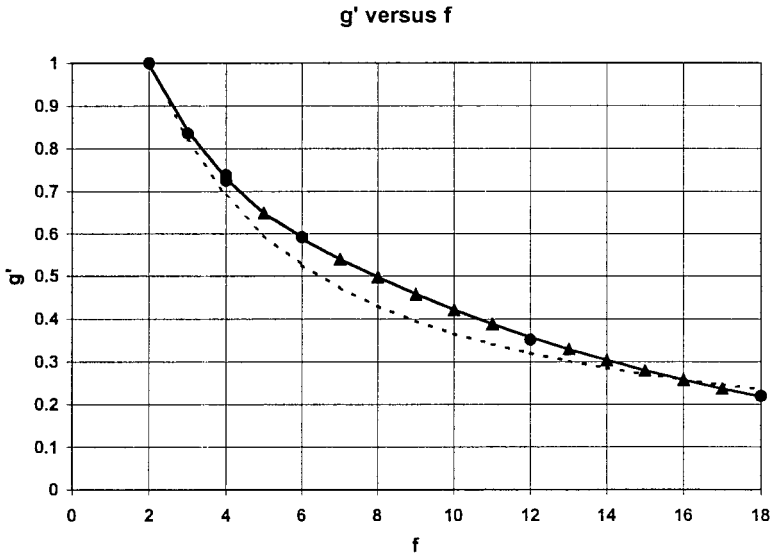

Figure 4 g' versus f: ●, directly obtained from the experimental data of Figure 3; ▲, obtained from eqs. (22) and (23); —, eqs. (22) and (23); ---, eq. (3).

where the κ_j are component detector response constants and the $A_{\mathrm{DRI},j}$ are component areas.

In this work, m_{exp} is considered the true value. In addition, all components are assumed to have the same value of κ_j.

Any significant difference between these mass estimates is considered a signal that a problem such as polymer deposition in the column, an error in detector response constant, or inadequate curve fitting exists.

5. The heights of the DV chromatogram are converted to specific viscosity and the whole polymer intrinsic viscosity $[\eta]$ is calculated from the total area under the DV (η_{sp}) chromatogram (A_{DV}) and m_{exp}. This value is needed for a later data check.

$$[\eta] = \frac{A_{\mathrm{DV}}}{m_{\mathrm{exp}}} \tag{13}$$

6. The heights of the LS chromatogram are converted to excess Raleigh factors. Then, assuming that the scattering function $P(\theta)$ is unity and that the term A_2c_i in eq. (7) is zero, whole polymer weight-average molecular weight M_w is calculated from the total area under the LS ($R(\theta)$) chromatogram (A_{LS}) and m_{exp}. This value is needed for a later data check.

$$M_w = \frac{A_{\mathrm{LS}}}{K_{\mathrm{LS}} m_{\mathrm{exp}}} \tag{14}$$

Peak retention volumes and standard deviations are compared for the Gaussian component chromatograms obtained from the fitting procedure of step 3 above. Two types of comparisons are computed: between duplicates and among different detectors. Significant differences between duplicates indicate a precision problem in the fitting. Differences among different detectors for the peaks of the components show the interdetector volume effect.

7. Component masses m_j are calculated from the area under the component DRI chromatograms, the total area under the corresponding whole DRI chromatogram, and the experimental value of the total mass injected.

$$m_j = \frac{A_{\mathrm{j,DRI}}}{A_{\mathrm{DRI}}} m_{\mathrm{exp}} \tag{15}$$

8. Component intrinsic viscosity values $[\eta]_j$ are obtained from the area under the component DV chromatograms $A_{\mathrm{DV},j}$ and the component mass injected m_j.

$$[\eta]_j = \frac{A_{j,\mathrm{DV}}}{m_{j,\mathrm{exp}}} \tag{16}$$

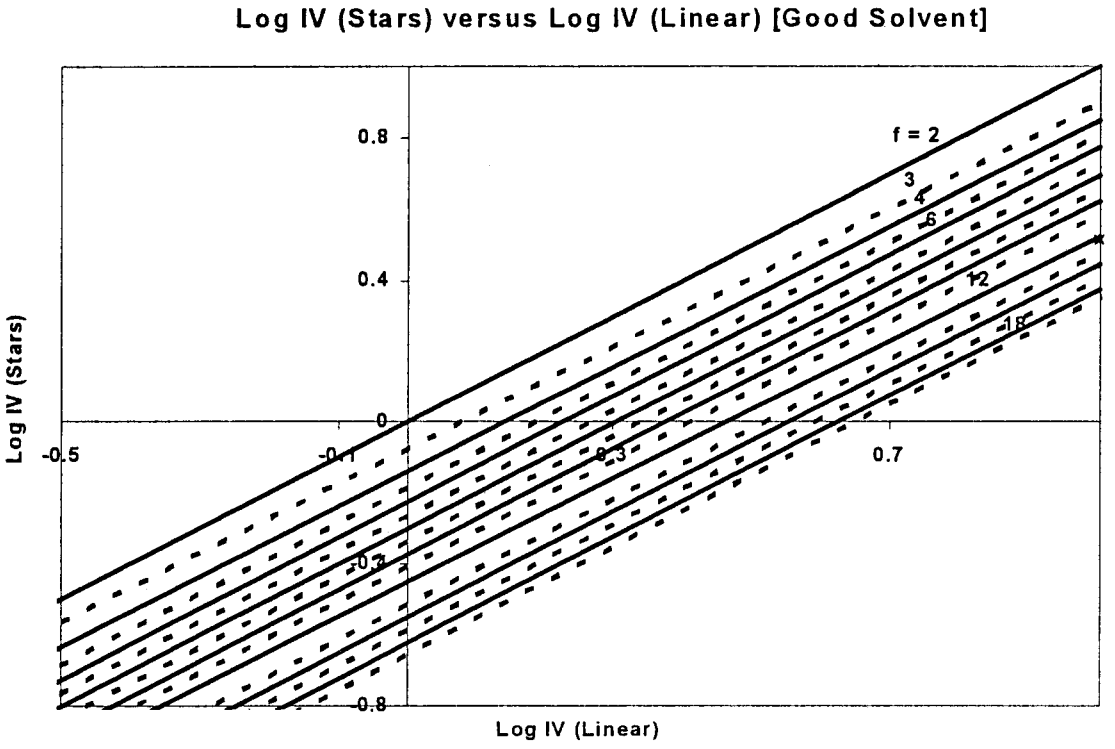

Figure 5 The same as Figure 3 except including results for interpolated values of f and extending only to $f = 18$. (The lines for $f = 12$ and $f = 13$ are indistinguishable on this figure.)

9. Whole polymer intrinsic viscosity values $[\eta]_{SC}$ are obtained from the weighted sum of the component intrinsic viscosity values and compared to the values ($[\eta]$) obtained from step 5 above.

$$[\eta]_{SC} = \sum_{i=1}^{n} \frac{A_{j,\mathrm{DRI}}}{A_{\mathrm{DRI}}}[\eta]_j \tag{17}$$

10. Significant differences between $[\eta]$ and $[\eta]_{SC}$ likely indicate a problem with the component fitting of the DV chromatogram.
11. Component weight-average molecular weight values $M_{w,j}$ are obtained from the area under the component LS chromatograms $A_{\mathrm{LS},i}$ and the component mass injected m_j.

$$M_{w,j} = \frac{A_{j,\mathrm{LS}}}{K_{\mathrm{LS}} m_j} \tag{18}$$

12. Whole polymer weight-average molecular weight values $M_{w,\mathrm{SC}}$ are obtained from the weighted sum of the component weight-average molecular weight values $M_{w,j}$ and are compared to the values (M_w) obtained from step 6 above.

$$M_{w,SC} = \sum_{i=1}^{n} \frac{A_{j,\mathrm{DRI}}}{A_{\mathrm{DRI}}} M_{w,j} \tag{19}$$

Significant differences between M_w and $M_{w,\mathrm{SC}}$ likely indicate a problem with the component fitting of the LS chromatogram.

At this point g', $[\eta]_{br,M}$, and $[\eta]_{\mathrm{lin},M}$ can be calculated for each component.

The Component Chromatogram Method Using Only the DRI and DV Data

Determining the intrinsic viscosity of a linear polymer of the same molecular weight as that of the branched polymer, without the light-scattering detector to measure molecular weight, is the main problem.

When universal calibration is used then the intrinsic viscosity of a linear polymer of the same molecular size (same peak retention volume) $[\eta]_i^*$

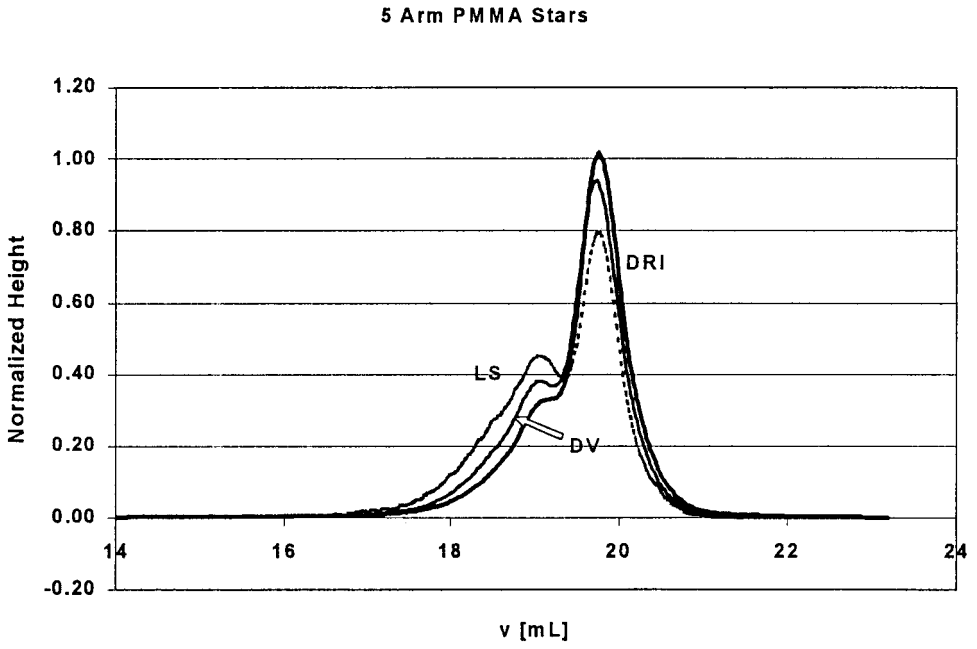

Figure 6 Normalized chromatograms from the differential refractive index (DRI), differential viscometer (DV), and light-scattering (LS) detectors.

can be obtained for a narrow distribution polymer. Scholte[18] showed how g_i' could be calculated as

$$g_i' = \left(\frac{[\eta]_{br,i}}{[\eta]_i^*}\right)^{a+1} \tag{20}$$

It can be similarly shown that $[\eta]_{\mathrm{lin},i}$ can be expressed in terms of $[\eta]_{br,i}$ and $[\eta]_i^*$:

$$[\eta]_{\mathrm{lin},i} = \left(\frac{[\eta]_i^*}{[\eta]_{br,i}}\right)^{a} [\eta]_i^* \tag{21}$$

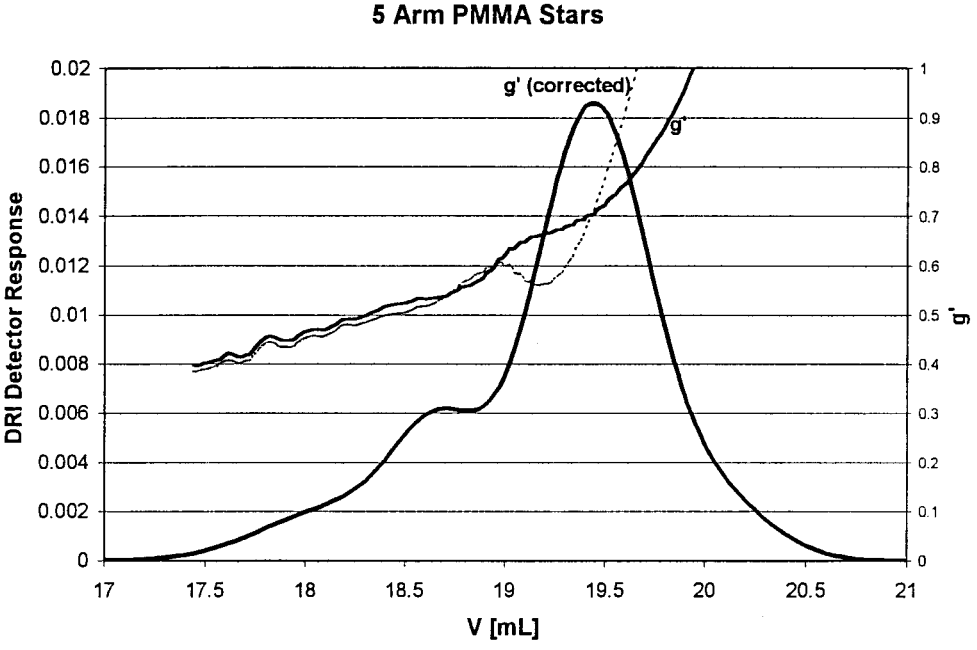

Figure 7 g' versus retention volume (v) for a sample of five-arm PMMA stars showing uncorrected values and values corrected for axial dispersion [eqs. (9) and (10)].

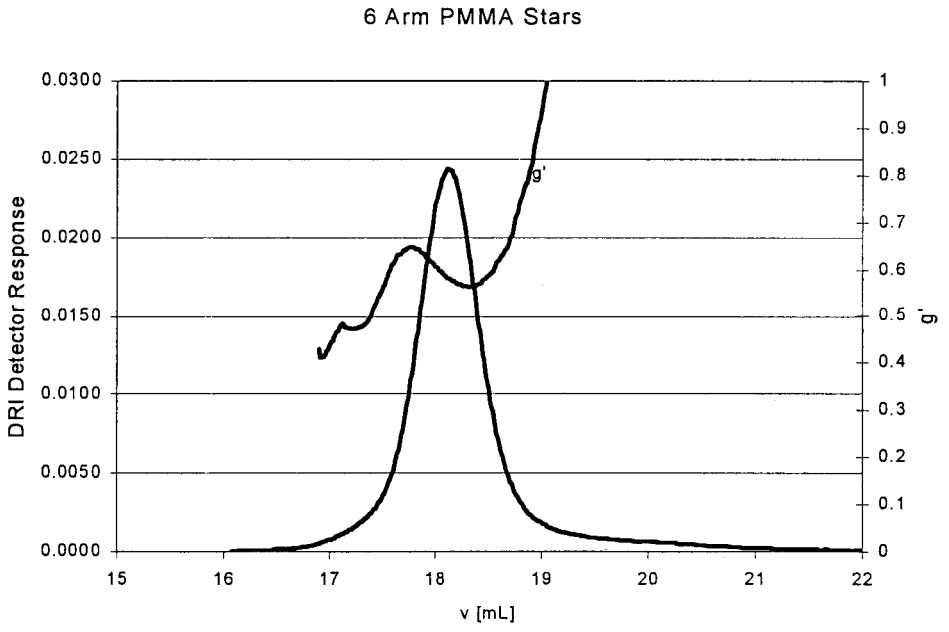

Figure 8 g' versus retention volume (v) uncorrected for axial dispersion for a sample of six-arm PMMA stars.

$[\eta]_i^*$ is obtainable from fitting whole polymer intrinsic viscosity versus retention volume for a series of narrow distribution linear homopolymer standards and solving for the value corresponding to v_i and the $[\eta]_{br,i}$ is directly measured by the DV. Therefore, as before, $[\eta]_{\mathrm{lin},i}$, $[\eta]_{br,i}$, and g'_i can be readily obtained.

EXPERIMENTAL

SEC detectors were arranged in series in the following order: 757 Spectroflow spectrophotometric detector (UV), Precision Detectors PD2000 15 and 90° light-scattering (LS) detector, Viscotek H502A differential viscometer (DV), and Waters 410 dif-

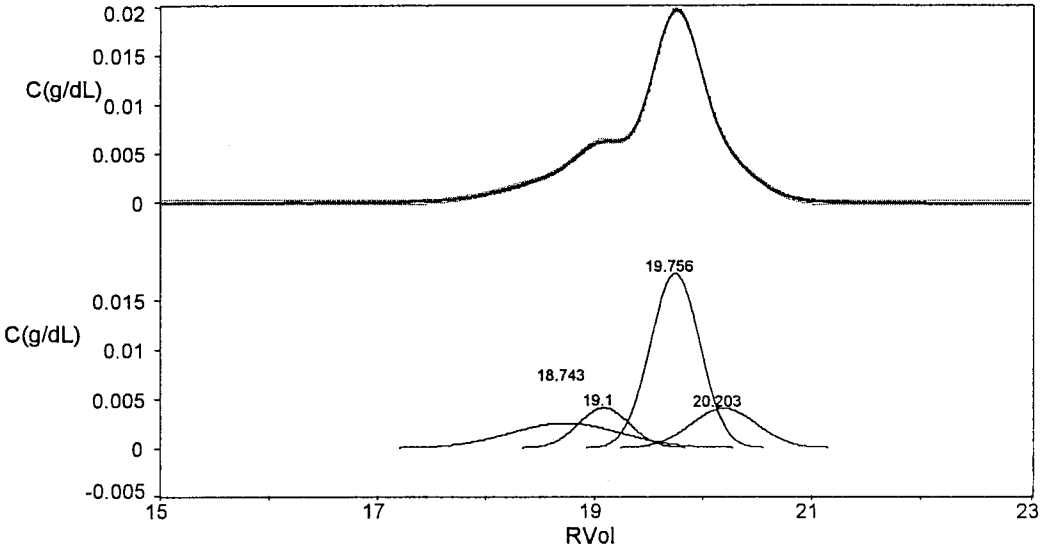

Figure 9 DRI chromatogram of a sample of five-arm PMMA fit as the sum of Gaussian component chromatograms.

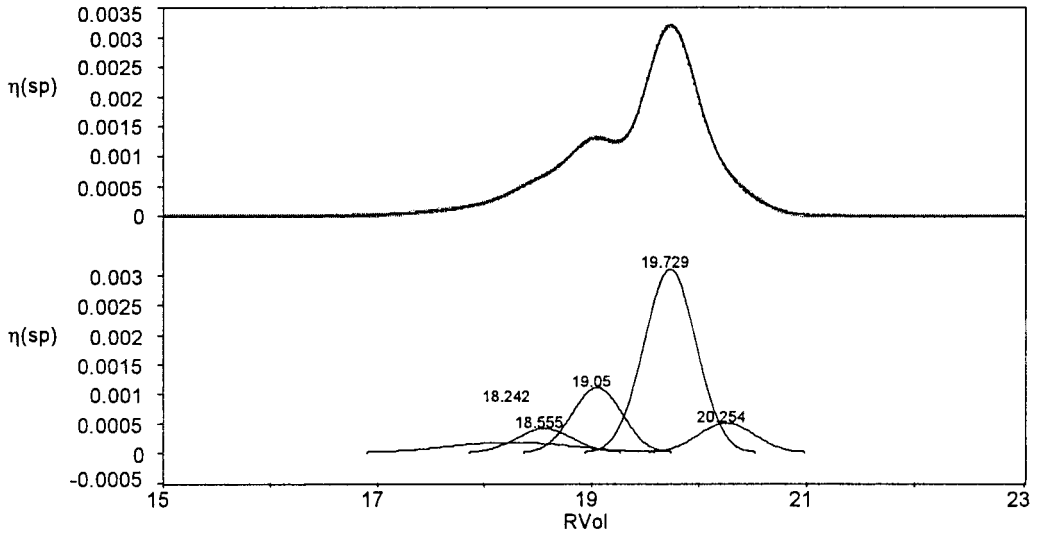

Figure 10 DV chromatogram of a sample of five-arm PMMA fit as the sum of Gaussian component chromatograms.

ferential refractive index (DRI) detector (Waters Associates, Milford, MA). The columns LS, DV, and DRI detector temperatures were 35.0 ± 0.1°C. Specific refractive index increments (*dn/dc*) calculated from the integrated DRI response and the mass of sample injected were in agreement with those for the linear homopolymers (PMMA = 0.078 mL/g for a 670 nm light source). Berkowitz[19] determined the *dn/dc* value for PMMA at 633 nm to be 0.083 and at 546 nm to be 0.087. These values extrapolate to 0.081 at 670 nm, not significantly different from our measured value. The eluent was HPLC-grade uninhibited tetrahydrofuran, delivered at a nominal flow rate of 1.0 mL/min. Flow rate corrections were made from the retention volume of acetone, added to the sample solvent at a concentration of 0.2% (v/v). Columns were three Plgel mixed-C (7.5 × 300 mm; Polymer Laboratories). A universal calibration curve was constructed using 16 narrow molecular weight distribution polystyrene standards (Polymer Laboratories) ranging from MW 580 to

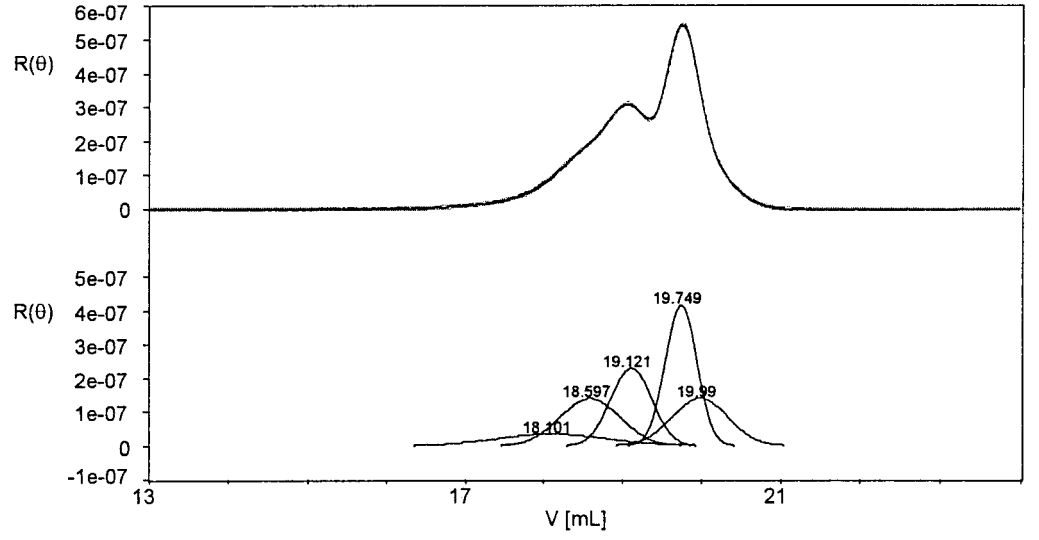

Figure 11 LS chromatogram of a sample of six-arm PMMA fit as the sum of Gaussian component chromatograms.

Table II g' Values for Replicate Analyses of the 5-Arm Star Sample

	g' from eq. (22): 0.649		
		Peaks	
	Main Peak	3 + 4 + 5	Total Area
	0.987	0.675	0.555
	0.875	0.642	0.573
	0.654	0.563	0.678
	0.837	0.563	0.563
Average	0.838	0.611	0.592

2,300,000. Star samples were injected in a volume of 100 μL at a concentration of 1.5 mg/mL.

RESULTS AND DISCUSSION

Establishing Correlations Relating the Number of Arms per Star (f) to SEC Data

Grest et al.[14] screened the published literature on the analysis of star polymers with particular attention to the polydispersity of the samples analyzed. Returning to the original references he listed (Table I in Grest et al.[14]) and plotting the data according to eq. (5) resulted in Figure 3. Each of these sets of data is for good solvents and was fit by linear regression to arrive at the values of g' listed in Table I as "g' This Study." These values were plotted versus f, as shown in Figure 4. Values of g' at values of f not available from the references needed to be obtained by interpolation. Combining eqs. (3) and (4) with $\epsilon = 0.79$ provides the dashed line in this plot. Because of the poor fit to the data, it was decided to fit the data by two empirical equations and to interpolate using those. The equations used are as follows:

$$2 \leq f \leq 6$$

$$\log g' = 0.1800 - 0.1020f + 0.005696f^2 \quad (22)$$

$$6 < f \leq 18$$

$$\log g' = -0.01617 - 0.03583f \quad (23)$$

Equations (22) and (23) are plotted as the solid line in Figure 4. The interpolated values of g' are shown in Table I along with the random walk values corresponding to the dashed line in Figure 2. Using the interpolated values, $[\eta]_{br,i}$–$[\eta]_{\mathrm{lin},i}$ plots corresponding to eq. (5) at f values not obtainable experimentally were calculated, assuming a slope of unity. The final plots for eq. (5) at values of f to 18 are shown in Figure 5. Figures 4 and 5 thus show the final correlations required to obtain values of f from SEC data. The fits represented by eqs. (22) and (23) are quite good: data points are all "on" the solid line of Figure 4. The main uncertainty then originates from determining g' for the unknown. For example, if the plot

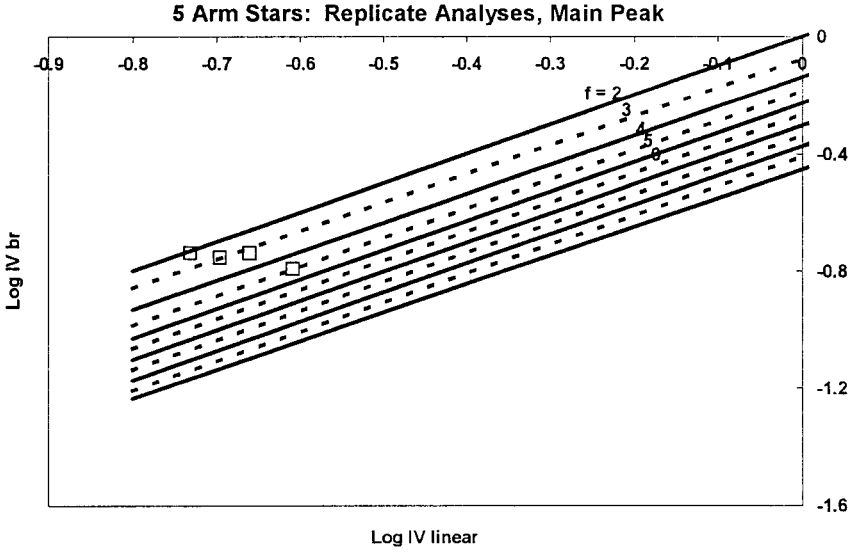

Figure 12 $[\eta]_{br,i}$–$[\eta]_{\mathrm{lin,i}}$ plot for replicate analyses of a sample of five-arm stars: results of using the main component peak in the method of component chromatograms.

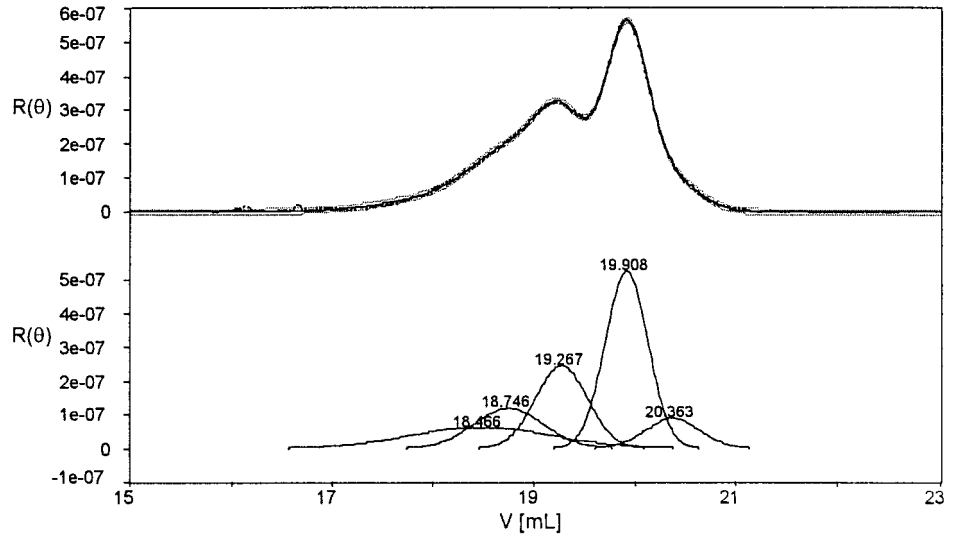

Figure 13 LS chromatogram of a sample of six-arm PMMA fit as the sum of Gaussian component chromatograms showing different component curves than its duplicate shown in Figure 11.

was used for a poor solvent rather than a good solvent, an error in g' of as high as 10% would be expected from this cause alone (based on the published values of g' in theta solvent) for f values of 4 to 6. It can be seen that this would correspond to an error in f of less than ± 1. In this work we are quite satisfied with that level of precision, and avoid the uncertainty introduced by not knowing the value of ϵ across the molecular size distribution and the application of eq. (4).

Application of the Conventional Approach

Figure 6 shows three normalized chromatograms, one from each of the three detectors, for a sample synthesized as a five-arm PMMA star. The bimodal appearance of these chromatograms leads to the suspicion that there are by-products accompanying the main product.

Figure 7 shows the values of local g' across the chromatogram using uncorrected values of intrinsic viscosity and weight-average molecular weight in eqs. (1) and (2). Also shown are the values of local g' after axial dispersion correction using eqs. (9) and (10). The local g' values vary from about 0.2 at the highest molecular weights to as high as unity (corresponding to linear polymer) at the lowest molecular weights. Axial dispersion correction has very little effect for any reasonable values of σ. The values of g' appear reasonable for a five-arm star when they plateau over the width of the main peak at a value of 0.65 to 0.68; there is variation of g' across the chromatogram, particularly at long and short retention volumes, although all values of g' are rational (i.e., values range between 0 and 1.0).

Figure 8 shows a similar plot to that of Figure 7, except that the sample has a much narrower molecular weight distribution and the main product is expected to be a six-arm PMMA star. The variation of g' (uncorrected for axial dispersion) is shown and appears very erratic. Now, unrealistic values of g' exceed unity at lower molecular weights. Although the results of analyzing the sample shown in Figure 7 are at least possible, the results for this sample are irrational and not acceptable.

Application of the Method of Component Chromatograms

Figures 9–11 show the fitting of each of the three chromatograms (one from each of the three detectors present) for the five-arm PMMA star sample by the sum of component chromatograms. Also shown in the top part of each figure is the superposition of the chromatogram obtained as the sum of component chromatograms and the experimental chromatogram of the whole sample. The DRI chromatogram was fit as the sum of four Gaussian chromatograms, whereas the DV and LS detectors, which are more sensitive at the low retention volumes, required five.

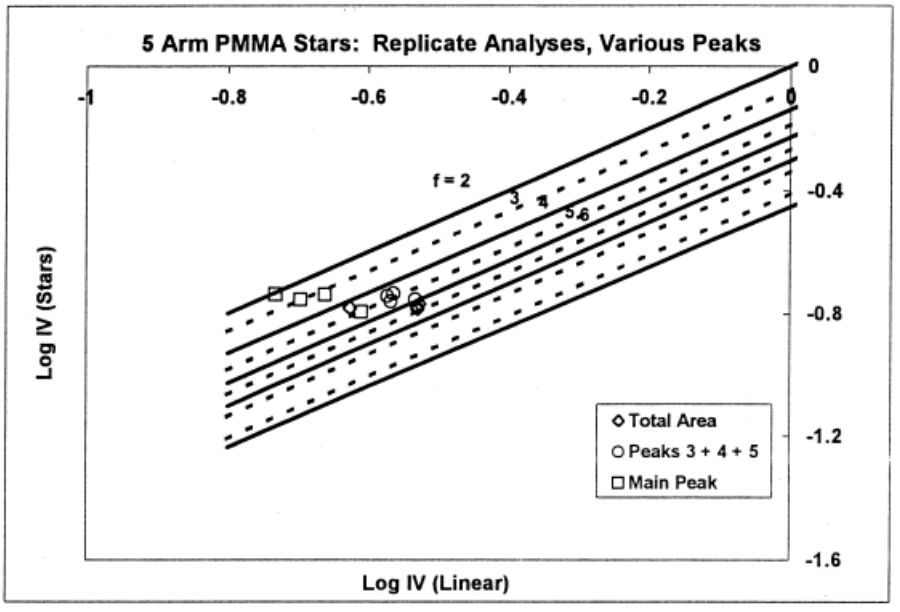

Figure 14 $[\eta]_{br,i}$–$[\eta]_{\mathrm{lin,i}}$ plot for replicate analyses of a sample of five-arm stars showing the results of using grouped component peaks as well as only the main component peak.

Table II shows the values of g' for this sample, calculated using only the chromatogram of the main component (the component peak with the greatest area). Results are poor: values of g' vary from 0.654 to almost unity for four replicate analyses of this sample. Figure 12 shows the same results superimposed on the plot corresponding to eq. (5). This plot demonstrates that the main source of variation is the value of the intrinsic viscosity of the corresponding linear polymer. This value is calculated from the value of M_w for the component , which in turn is obtained from the area under the component light-scattering chromatogram. The poor reproducibility was attributed to differences in how the light-scattering chromatograms were fit as the sum of component chromatograms for the different replicate analyses. Figures 11 and 13 confirm this as the cause. There is shown the light-scattering chromatograms together with their component chromatograms for the two replicates exhibiting extreme values of g'. We see that the main peak at approximately 19.8 mL is dramatically different in area for the two samples because the peak at about 20.0 mL is much larger in one case than that in the other. This example served to show the main limitation of the component chromatogram method.

That limitation is that a particular component chromatogram must correspond to the same molecules in the DRI, DV, and LS chromatograms. Accomplishing this feat is not trivial: the shape of the component chromatograms and the number of component chromatograms can be different for DRI, DV, and LS chromatograms because of their different sensitivities and different responses. One way of increasing the chance that the same molecules are included is to group component chromatograms. That is, for example, the latest eluting three-component peaks can be considered as one peak. Table II shows the result of combining these peaks (peaks 3, 4, and 5, numbering from left to right). The situation is dramatically improved. Values of g' for the four replicates now vary from 0.56 to 0.68. The extreme of this approach is to group all of the peaks together. The results of this action are shown in Table II. Interestingly, the result is not much different than when the last three peaks are grouped. This may indicate that these materials are more homogeneous than suspected or, more likely, that averaging effects are responsible.

Figure 14 summarizes the results on a $[\eta]_{br,i}$–$[\eta]_{\mathrm{lin},i}$ plot. There we see that grouping all of the peaks or examining only peaks 3, 4, and 5 indicates that the polymer has five to six arms.

Figures 15 and 16 show the component chromatograms of the six-arm PMMA DRI and LS chromatograms. The former yielded three components, whereas the latter (and the DV peak, not

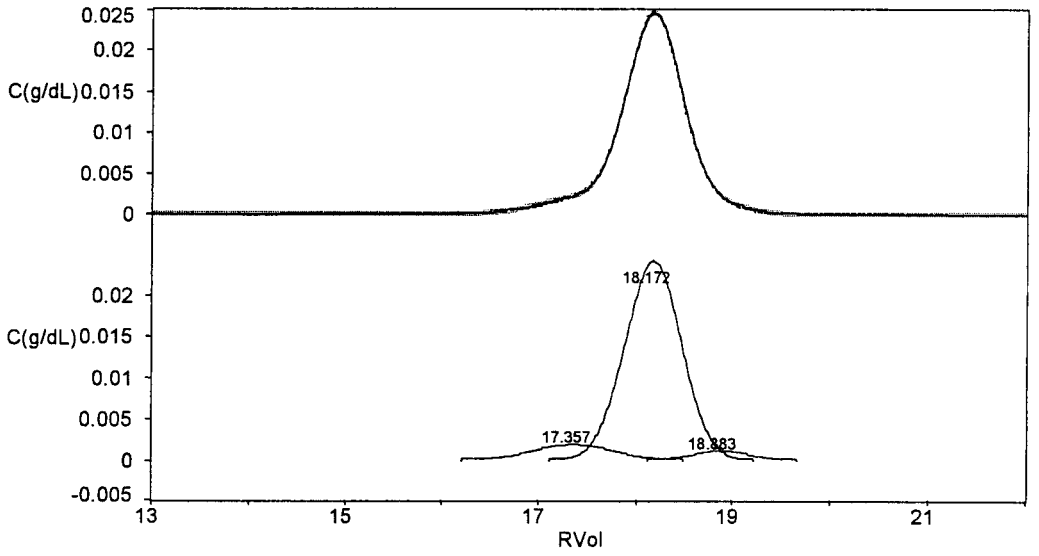

Figure 15 DRI chromatogram of a sample of six-arm PMMA stars fit as the sum of Gaussian component chromatograms.

shown) yielded four. Results were very similar to those obtained with the sample of five-arm PMMA stars. When only the main peak was used, poor reproducibility of the g' resulted. Here, as evident in Table III, values ranged from 0.66 to 0.8. Grouping of three of the component peaks or all of the peaks together greatly improved precision and accuracy. Figure 17 shows the results on a $[\eta]_{br,i}$–$[\eta]_{\mathrm{lin},i}$ plot. Also shown are the results of grouping only the last two peaks (peaks 3 and 4). These results show that the sample probably contains from five to six arms per star.

Results of Using the Component Chromatogram Method with Only DRI and DV Data

Figure 18 shows a $[\eta]_{br,i}$–$[\eta]_{\mathrm{lin},i}$ plot for four different samples of six-arm PMMA stars (not replicates as in the previous sections of this study). All of these samples had very narrow molecular

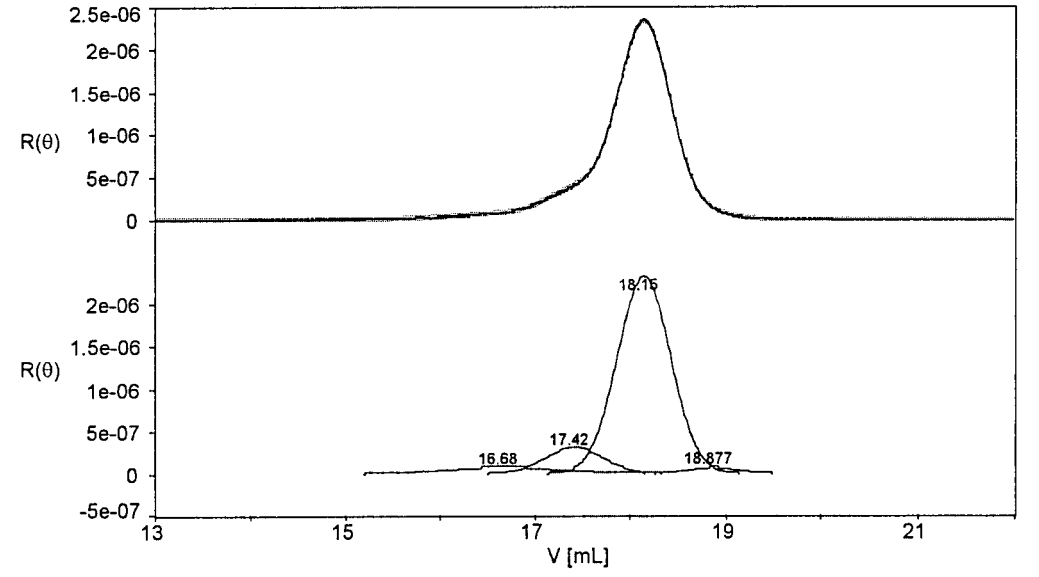

Figure 16 LS chromatogram of a sample of six-arm PMMA stars fit as the sum of Gaussian component chromatograms.

Table III g' Values for Replicate Analyses of the 6-Arm Star Sample

	g' from eq. (22): 0.593			
	Main Peak	Peaks 3 + 4	Peaks 2 + 3 + 4	Total Area
	0.679	0.672	0.647	0.627
	0.681	0.671	0.636	0.617
	0.802	0.778	0.609	0.601
	0.656	0.650	0.627	0.602
Average	0.704	0.693	0.630	0.612

weight distributions and were analyzed on a dual detector SEC (only a DRI and DV detector was used). Results for these samples were about the same, regardless of whether only the main peak was used or whether the three-component peaks were all grouped together. Three of the four samples show that the best estimate of the number of arms per molecule is the expected six. One shows a low value of four arms per molecule.

CONCLUSIONS

Two correlations were shown to provide a basis for determining the number of arms per molecule for stars from multidetector SEC analysis. The correlation of g' versus f and the correlation of $\log[\eta]$ of the branched polymer versus $\log[\eta]$ of the linear polymer of the same molecular weight. The latter correlation was particularly useful for diagnosing which chromatogram (i.e., which detector response) was providing the main source of error in the correlation of g' and f.

The conventional interpretation method resulted in values of g' across the chromatograms but the results appeared increasingly uncertain as the molecular weight polydispersity of the samples decreased. Axial dispersion correction had no significant effect on the results.

The component chromatogram method circumvented both determination of interdetector volume and axial dispersion correction. However, a significant limitation was that the chromatograms of the components had to encompass exactly the same molecules for each detector's chromatogram. The degree to which this could be attained depended on how accurately each detector's chromatogram was represented by the component chromatograms. The shape, position, and area of each component for each detector's chromatogram was important. Using a Gaussian shape assumes that each different species present has an extremely narrow molecular weight distribution (and degree of branching) so that only axial dispersion was causing the component chromatogram to deviate from a "spike." However, it was found that, in general, it was necessary to

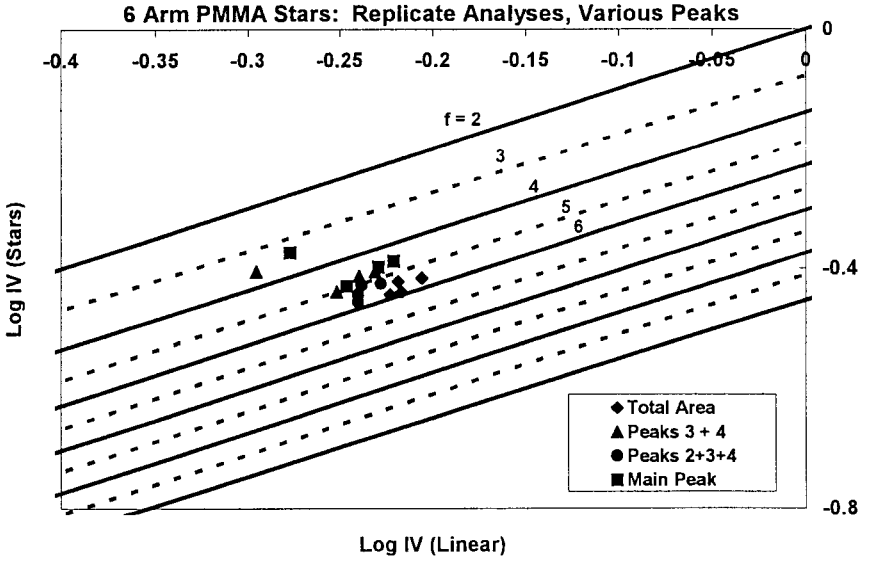

Figure 17 $[\eta]_{br,i}$–$[\eta]_{\mathrm{lin,i}}$ plot for replicate analyses of a sample of six-arm stars showing the results of using grouped component peaks as well as only the main component peak.

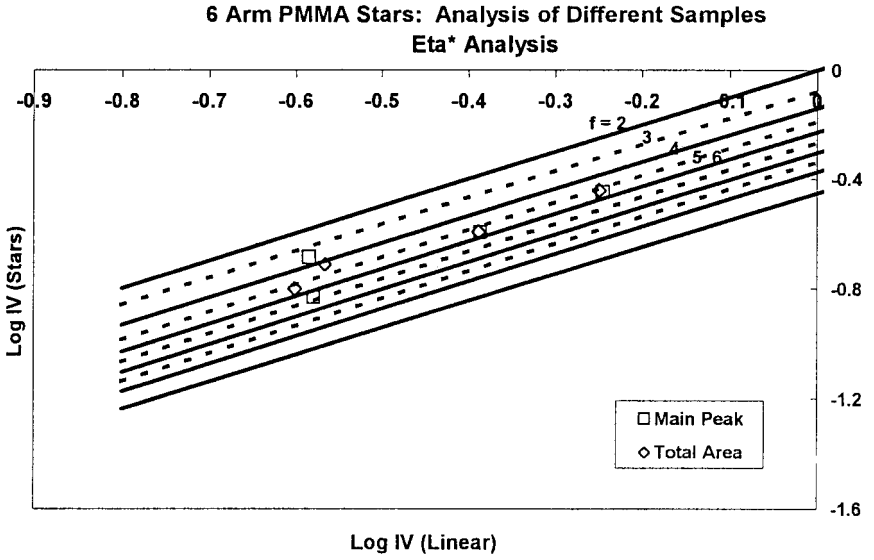

Figure 18 $[\eta]_{br,i}$–$[\eta]_{\mathrm{lin,i}}$ plot for analyses of five different samples of six-arm stars showing the results of using all component peaks grouped together as well as only the main component peak using data from only a DRI and a DV detector.

group component chromatograms to obtain reasonable results. For the five- and six-arm stars initially examined it was found that taking the whole area under each detector's chromatograms provided about the same results as grouping a smaller number of component chromatograms. Results showed that the number of arms represented by the product was between five and seven when the actual values were expected to be between five and six.

The method of calculating f without the use of the light-scattering detector appears very promising. The fact that DV and LS detectors are more sensitive than the DRI detectors to high molecular weights is a major complication because it leads to great uncertainty in specifying the number of components when detailed kinetic information is not available.

The authors gratefully acknowledge the synthetic work of Alix Andre of Kodak Research Laboratories.

REFERENCES

1. Roovers, J. in Encyclopedia of Polymer Science Engineering, 2nd ed.; Kroschwitz, J. I., Ed.; Wiley-Interscience: New York, 1985; Vol. 2, pp 478–499.
2. Baner, B. J.; Fetters, L. J. Rubber Chem Tech 1978, 51, 406.
3. Hadjichristidis, N.; Guyot, A.; Fetters, L. J. Macromolecules 1978, 11, 668.
4. Long, T. E.; Kelts, L. W.; Turner, S. R.; Wesson, J. A.; Mourey, T. H. Macromolecules 1991, 24, 1431.
5. Deng, H.; Kanaoka, S.; Sawamoto, M.; Higashimura, T. Macromolecules 1996, 29, 1772.
6. Kennedy, J. P.; Jacob, S. Acc Chem Res 1998, 31, 835.
7. Heise, A.; Hedrick, J. L.; Frank, C. W.; Miller, R. D. J Am Chem Soc 1999, 121, 8647.
8. Matyjaszewski, K.; Miller, P. J.; Pyun, J.; Kickelbick, G.; Diamanti, S. Macromolecules 1999, 32, 6526.
9. Angot, S.; Murthy, K. S.; Taton, D.; Gnanou, Y. Macromolecules 2000, 33, 7261.
10. Wang, J.-S.; Matyjaszewski, K. J Am Chem Soc 1995, 117, 5614.
11. Kraus, A.; Robello, D. R. Polym Prepr (Am Chem Soc Div Polym Chem) 1999, 40, 413.
12. Percec, V.; Barboiu, B.; Kim, H. J. J Am Chem Soc 1998, 120, 305.
13. Mourey, T. H. Balke, S. T. in Chromatography of Polymers, Provder, T., Ed.; ACS Symposium Series 521; American Chemical Society: Washington, DC, 1993; pp 180–198.
14. Grest, G. S.; Fetters, L. J.; Huang, J. S.; Richter, D. in Star Polymers: Experiment, Theory, and Simulation (Adv Chem Phys XCIV); Prigogine, I.; Rice, S. A., Eds.; Wiley: New York, 1996; pp 67–163.
15. Zimm, B. H.; Stockmayer, W. H. J Chem Phys 1949, 17, 1301.

16. Jackson, C.; Frater, D. J.; Mays, J. W. J Polym Sci Part B: Polym Phys 1995, 33, 2159.
17. Hamielec, A. E. Pure Appl Chem 1982, 54, 293.
18. Scholte, Th. G.; Meijerink, N. L. J. Br Polym J 1977, June, 133.
19. Berkowitz, S. A. J Liq Chromatogr 1983, 6, 1359.
20. Khasat, N.; Pennisi, R. W.; Hadjichristidis, N.; Fetters, L. J. Macromolecules 1988, 21, 1100.
21. Roovers, J. E. L.; Bywater, S. Macromolecules 1972, 5, 384.
22. Hadjichristidis, N.; Roovers, J. E. L. J Polym Sci Part B: Polym Phys 1974, 12, 2521.
23. Toporowski, P. M.; Roovers, J. J Polym Sci Part A 1986, 24, 3009.
24. Zhou, L. L.; Hadjichristidis, N.; Toporowski, P. M.; Roovers, J. Rubber Chem Technol 1992, 65, 303.
25. Roovers, J.; Zhou, L. L.; Toporowski, P. M.; van der Zwan, M.; Iatrou, H.; Hadjichristidis, N. Macromolecules 1993, 26, 4324.
26. Roovers, J.; Toporowski, P.; Martin, J. Macromolecules 1989, 22, 1897.